JOURNAL OF CATALYSIS 116, 119–129 (1989)

Kinetic Simulation of Ammonia Synthesis Catalysis

J. A. DUMESIC*,[1] AND A. A. TREVIÑO†

*Department of Chemical Engineering, University of Wisconsin, 1415 Johnson Drive, Madison, Wisconsin 53706, and †Shanahan Valley Associates, 5118 Sherwood Road, Madison, Wisconsin 53711

Received September 2, 1988; revised October 20, 1988

Kinetic simulation studies were carried out and showed that kinetic and spectroscopic data collected on iron single crystals under ultrahigh vacuum conditions can be used to predict the rate of ammonia synthesis over a commercial iron catalyst in a plug-flow reactor operating under industrial reaction conditions (i.e., 720 K, 107 atm). The results agree with earlier calculations by P. Stoltze and J. K. Norskov [Surf. Sci. Lett. **197,** L230 (1988); *Phys. Rev. Lett.* **55,** 2502 (1985); *Phys. Scr.* **36,** 824 (1987); *J. Catal.* **110,** 1 (1988)]. Furthermore, the kinetic simulations confirm the fact that the dissociation of molecular dinitrogen precursor species is a slow step in the mechanism; however, other steps may also become slow depending on reaction conditions. Atomic nitrogen appears to be the most abundant reactive intermediate on the iron surface, except at the reactor inlet, where a variety of adsorbed species may compete for surface sites. Finally, the kinetic simulation results are also shown to describe the performance of iron catalysts in laboratory reactors operating at pressures from 1 to 20 atm.

INTRODUCTION

An understanding of the kinetics of chemical processes on solid surfaces has been, and remains today, one of the most important areas of heterogeneous catalysis. In general, the information obtained by surface scientists on single crystal surfaces under ultrahigh vacuum conditions should be combined with studies of high-surface-area catalysts under reaction conditions to provide the knowledge needed to postulate realistic reaction mechanisms and to estimate the corresponding rate constants.

Progress in this direction has been slow, at least in part due to the difficulty in analyzing quantitatively complex reaction mechanisms. During the past several years, we have been developing numerical techniques at the Unversity of Wisconsin and Shanahan Valley Associates to explore the quantitative aspects of reaction mechanisms that do not make a priori assumptions about rate-determining steps or most abundant surface intermediates. The use of such kinetic simulations in directing experimental research in catalysis is discussed elsewhere in a preliminary fashion (*1*). The objective of the present paper is to use these numerical techniques to probe the kinetics of ammonia synthesis over iron catalysts.

There has been some disagreement (*2, 3*) as to whether rates of surface reactions on single crystal iron surfaces under ultrahigh vacuum conditions [e. g., (*4–16*)] can be used to predict rates of ammonia synthesis over high-surface-area iron catalysts under industrial reaction conditions. According to Stoltze and Norskov (*3, 17–19*), it appears possible to extrapolate, with considerable success, the results from single crystal studies to predict the performance of an industrial, potassium-promoted ammonia synthesis catalyst. In contrast, Bowker *et al.* (2, 20) report that this extrapolation predicts rates of ammonia synthesis that are 40 times lower than those measured under industrial conditions.

Regardless of which of the two research groups is correct, it should be noted that it

[1] Author to whom correspondence should be addressed.

0021-9517/89 $3.00

is rather impressive to be able to extrapolate over 11 orders of magnitude in pressure (from 10^{-6} Torr to 100 atm) to predict the rate of ammonia synthesis within a factor of 40. Despite this fact, the origin of the difference between extrapolations of these two groups remains unclear. A significant difference between the approach of Stoltze and Norskov and the method of Bowker *et al.* is that the former group assumed that the formation of atomic, chemisorbed nitrogen from a molecular precursor state was rate determining, whereas Bowker *et al.* made no assumptions regarding the nature of rate-determining steps. It is possible that this assumption and differences in the numerical methods used by these authors are responsible for the different results reported.

It will be shown that the kinetic simulations of the present work are in agreement with the calculations of Stoltze and Norskov. Specifically, the ammonia concentration in the effluent of an industrial reactor operating at 107 atm can be predicted with a relative uncertainty of less than 15%. Moreover, we will show that the same kinetic model predicts well the rate of ammonia synthesis over iron catalysts in laboratory reactors operating at pressures from 1 to 20 atm. Regarding the conclusions of Bowker *et al.*, it appears that these authors used a value for the active site density that was too low by a factor of about 50.

KINETIC MODEL FORMULATION

The kinetic mechanism employed by Stoltze and Norskov is depicted below:

$$N_2 + * = N_2* \quad (1)$$

$$N_2* + * = 2N* \quad (2)$$

$$H* + N* = NH* + * \quad (3)$$

$$NH* + H* = NH_2* + * \quad (4)$$

$$NH_2* + H* = NH_3* + * \quad (5)$$

$$NH_3* = NH_3 + * \quad (6)$$

$$H_2 + 2* = 2H* \quad (7)$$

These authors assumed that step (2) was rate determining and that all species were competively adsorbed. They used the data of Ertl and co-workers (*4, 7, 8, 12–16*) to estimate the rate constants for this step, and spectroscopic data to estimate the equilibrium constants for the remaining steps. Although Stoltze and Norskov assumed in their calculations that step (2) was rate determining, they also estimated the rate constants for step (3). We have used these latter estimates in our kinetic simulations of the complete reaction network.

Table 1 summarizes our estimates of the rate constants from the work of Stoltze and

TABLE 1

Rate Constants for Model of Stoltze and Norskov

Step	Forward rate constant		Reverse rate constant	
	Preexponential factor	Activation energy (kJ/mol)	Preexponential factor	Activation energy (kJ/mol)
1	3.33×10^3 Torr^{-1} s^{-1}	0.0	1.87×10^{14} s^{-1}	43.1
2	4.29×10^9 s^{-1}	28.5	1.32×10^9 s^{-1}	155.0
3	1.83×10^9 s^{-1}	81.3	1.15×10^7 s^{-1}	23.2
4	1.31×10^{13} s^{-1}	36.4	1.38×10^{12} s^{-1}	0.0
5	3.88×10^{13} s^{-1}	38.7	2.33×10^{13} s^{-1}	0.0
6	3.67×10^{12} s^{-1}	39.2	2.38×10^5 Torr^{-1} s^{-1}	0.0
7	9.23×10^3 Torr^{-1} s^{-1}	0.0	3.24×10^{13} s^{-1}	93.8

TABLE 2

Rate Constants for Model of Bowker *et al.* (Case 1)

Step	Forward rate constant		Reverse rate constant	
	Preexponential factor	Activation energy (kJ/mol)	Preexponential factor	Activation energy (kJ/mol)
1	3.85×10^3 Torr^{-1} s^{-1}	0.0	1.58×10^{10} s^{-1}	46.0
2	2.63×10^6 s^{-1}	31.3	2.63×10^{12} s^{-1}	199.0
3	1.05×10^{12} s^{-1}	64.9	1.66×10^{12} s^{-1}	18.8
4	8.32×10^{11} s^{-1}	64.9	1.66×10^{12} s^{-1}	18.8
5	6.61×10^{12} s^{-1}	64.9	1.66×10^{12} s^{-1}	18.8
6	1.00×10^{13} s^{-1}	52.7	2.43×10^4 Torr^{-1} s^{-1}	0.0
8	3.85×10^5 Torr^{-1} s^{-1}	0.0	1.58×10^{13} s^{-1}	0.0
9	2.63×10^{12} s^{-1}	0.0	2.63×10^{12} s^{-1}	92.0

Norskov. We have combined their reported values of the rate constants for steps (2) and (3) and the equilibrium constants for steps (1) and (4)–(7) at 723 K with the reported standard enthalpy changes for each step, to estimate the preexponential factors and activation energies given in Table 1. In this estimate, we have assumed for steps (1) and (4)–(7) that the activation energy is equal to zero in the exothermic direction. It should be noted that the true temperature dependence of the rate and equilibrium constants is slightly more complex than the Arrhenius form used in the present paper, due to the temperature dependence of the partition functions. Stoltze and Norskov have used this more complete temperature dependence, and we have simply matched an Arrhenius form of the rate constants to their values at 723 K (a typical ammonia synthesis reaction temperature).

The kinetic mechanism employed by Bowker *et al.* was essentially the same as that given above, with the exception that they allowed the dissociative adsorption of hydrogen to proceed via a precursor state (i.e., step 7 was replaced by steps 8 and 9). This mechanism is summarized below:

$$N_2 + * = N_2* \quad (1)$$

$$N_2* + * = 2N* \quad (2)$$

$$H* + N* = NH* + * \quad (3)$$

$$NH* + H* = NH_2* + * \quad (4)$$

$$NH_2* + H* = NH_3* + * \quad (5)$$

$$NH_3* = NH_3 + * \quad (6)$$

$$H_2 + * = H_2* \quad (8)$$

$$H_2* + * = 2H* \quad (9)$$

Two sets of activation energies and preexponential factors for these steps were reported by Bowker *et al.*, depending on how one interprets the temperature-programmed desorption data of Ertl and coworkers. The two sets of rate constants are summarized in Tables 2 and 3.

CONSISTENCY OF KINETIC RATE CONSTANTS

As noted above, three sets of kinetic rate constants (Tables 1–3) have been reported in the literature to be consistent with studies on iron single crystal surfaces. Two specific sets of experiments are particularly relevant in this respect: (i) sticking coefficient measurements and (ii) temperature-programmed desorption studies.

Ertl *et al.* (*16*) report that the initial sticking coefficient for dissociative adsorption of nitrogen on Fe(111) (the most active surface plane for ammonia synthesis) at 430 K

TABLE 3

Rate Constants for Model of Bowker *et al.* (Case 2)

Step	Forward rate constant		Reverse rate constant	
	Preexponential factor	Activation energy (kJ/mol)	Preexponential factor	Activation energy (kJ/mol)
1	3.85×10^3 Torr^{-1} s^{-1}	0.0	1.58×10^{10} s^{-1}	46.0
2	1.66×10^9 s^{-1}	31.4	1.66×10^9 s^{-1}	144.0
3	1.05×10^{11} s^{-1}	53.5	1.66×10^{12} s^{-1}	16.7
4	8.32×10^{10} s^{-1}	53.5	1.66×10^{12} s^{-1}	16.7
5	6.61×10^{11} s^{-1}	53.5	1.66×10^{12} s^{-1}	16.7
6	1.00×10^{13} s^{-1}	52.7	2.43×10^4 Torr^{-1} s^{-1}	0.0
8	3.85×10^5 Torr^{-1} s^{-1}	0.0	1.58×10^{13} s^{-1}	0.0
9	2.63×10^{12} s^{-1}	0.0	2.63×10^{12} s^{-1}	92.0

ranges from 5×10^{-6} on the clean surface to 4×10^{-5} on an optimally promoted potassium surface. When the aforementioned three sets of rate constants for steps (1) and (2) are extrapolated to 430 K, the following initial sticking coefficients are calculated (assuming steady state for adsorbed dinitrogen, as suggested by Ertl *et al.*): 1.4×10^{-5} for the model of Stoltze and Norskov, 1.2×10^{-4} for the model of Bowker *et al.* (Case 1), and 1.0×10^{-2} for Bowker *et al.* (Case 2). It is clear that the values for the models of Stoltze and Norskov and Bowker *et al.* (Case 1) are in general agreement with the reported low value of the sticking coefficient. The sticking coefficient predicted for Case 2 of Bowker *et al.* appears to be too high.

The apparent activation energy of the sticking coefficient for dissociative adsorption of nitrogen on potassium-promoted Fe(111) has been reported by Ertl *et al.* (*16*) to be −12 kJ/mol at temperatures near 400 K. The following values of this apparent activation energy are predicted by the three sets of rate constants for steps (1) and (2): −13 kJ/mol for the model of Stoltze and Norskov, −13 kJ/mol for the model of Bowker *et al.* (Case 1), and −0.5 kJ/mol for Bowker *et al.* (Case 2). The rate constants given by Stoltze and Norskov and Bowker *et al.* (Case 1) predict the proper temperature dependence of the sticking coefficient, while the rate constants of Bowker *et al.* (Case 2) are less successful in this respect.

Boszo *et al.* (*13*) have reported temperature-programmed desorption (TPD) spectra for nitrogen on Fe(111). The temperature at which the rate of desorption reaches a maximum (for a heating rate of 10 K/s) was determined to be in the range 850 to 890 K, with the higher temperatures being observed for lower intial surface coverages, as expected for second-order desorption. It is possible to simulate such a TPD experiment by solving simultaneously the two differential equations associated with time dependencies of the surface coverages by molecular and atomic nitrogen for a linear rate of temperature increase. The initial state for this problem is a surface at 77 K with a specific coverage by atomic nitrogen (ranging from 0.2 to 0.95). When the preexponential factors and activation energies reported by Stoltze and Norskov for steps (1) and (2) are used in such a dynamic simulation, the predicted peak temperature for the TPD experiment of Boszo *et al.* ranges from 820 to 870 K. The predicted peak temperatures for the rate constants of Bowker *et al.* range from 790 to 830 K for Case 1, and from 760 to 820 K for Case 2. It appears that the rate constants of Stoltze and Norskov and Bowker *et al.* (Case 1) are in

general agreement with the experimental TPD spectra, while the predicted peak temperatures for Bowker *et al.* (Case 2) seem to be too low.

Finally, the product of the equilibrium constants for the elementary steps of the reaction mechanism must give the overall equilibrium constant for the stoichiometric reaction (the equilibrium constant for each step appearing in this product raised to a power equal to the number of times that the step occurs in the overall reaction). At a temperature of 723 K, the overall equilibrium constant for ammonia synthesis (forming 2 mol of ammonia) is approximately 8×10^{-11} $Torr^{-2}$. The values predicted by the three sets of rate constants in Tables 1–3 are 9×10^{-11}, 5×10^{-11}, and 7×10^{-11}, respectively. At a total pressure of 107 atm and for a stoichiometric H_2/N_2 gas mixture, these equilibrium constants correspond to equilibrium ammonia concentrations of 17, 14, and 15%, respectively. These values are in general agreement with the ammonia concentration of 17% given by the true equilibrium constant for this reaction (without making corrections for nonideal gas behavior).

In summary, it appears that the rate constants estimated by Stoltze and Norskov and Bowker *et al.* (Case 1) are in general agreement with sticking coefficient measurements for dissociative nitrogen adsorption on potassium-promoted Fe(111) surfaces, with TPD spectra of nitrogen on Fe(111) crystals, and with the overall thermodynamics for ammonia synthesis. The rate constants of Bowker *et al.* (Case 2) do not appear to be as successful in reproducing the data obtained on single crystal surfaces. The next sections of this paper explore the utility of the above rate constants in explaining ammonia synthesis kinetics over a wide range of experimental conditions.

REACTOR SIMULATION

The experimental data that both of the above groups have attempted to explain were reported by Nielsen (*21*). One particular experimental point has been chosen by Bowker *et al.* as a test case. The reactor data for this point are summarized in Table 4.

TABLE 4

Reactor Data for Ammonia Synthesis (*21*)

Reactor type	Plug flow
Reactor volume	5 cm^3
Reactor pressure	107 atm
H_2-to-N_2 ratio	3 : 1
Space velocity	16,000 h^{-1}
Ammonia (% in effluent)	13.2

Other relevant data are needed to simulate the performance of the reactor: (1) the reactor was shown to operate as an isothermal plug-flow reactor; (2) the catalyst volume in the reactor was 2.5 cm^3 (the remaining volume was filled with a solid diluent); (3) the catalyst bed density was 2.5 g/cm^3; (4) the catalyst pellet size was 0.5 mm; (5) the space velocity was measured at normal temperature and pressure (NTP), and was based on the volume of the catalyst; and (6) the iron surface site density of the catalyst corresponded to about 6×10^{-5} mol/g [as estimated by CO chemisorption (*21*)]. Importantly, the ammonia synthesis kinetics under these conditions were not limited by transport phenomena (*21*).

We have modeled the above plug-flow reactor by a series combination of 10,000 well-mixed reactors. Actually, this simulation can be carried out without significant loss of precision using only 1000 well-mixed reactors. In each well-mixed reactor, we solve simultaneously the steady-state equations for all surface intermediates, the site balance on the catalyst surface, and the material balances for the gaseous species. Since there is a change in moles during reaction, it is perhaps useful to note the three material balances that we have used in each of the well-mixed reactors:

$$\frac{PS}{F} = \frac{(0.5)(P_{N_{2,in}} - P_{N_{2,out}})}{(1 - 2P_{N_{2,out}}/P)(1 - 2P_{N_{2,in}}/P)(R_{N_2})} \quad \text{(I)}$$

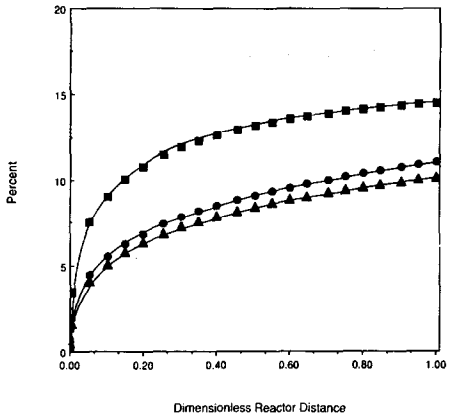

FIG. 1. Calculations of the ammonia concentration versus dimensionless longitudinal distance from reactor inlet: (●) Stoltze and Norskov, (▲) Bowker *et al.* (Case 1), (■) Bowker *et al.* (Case 2).

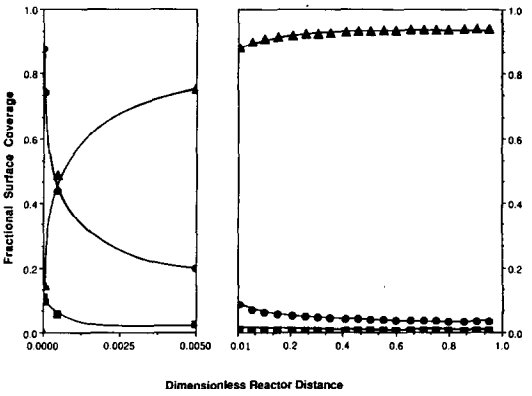

FIG. 3. Calculations, according to the model of Bowker *et al.* (Case 1), of fractional surface coverages by predominant adsorbed species versus dimensionless longitudinal distance from reactor inlet: (●) H*, (▲) N*, (■) N_2*.

$$P_{NH_{3,out}} = P - 4P_{N_{2,out}} \quad \text{(II)}$$

$$P_{H_{2,out}} = 3P_{N_{2,out}} \quad \text{(III)}$$

where P is the total pressure, S is the number of sites in each well-mixed reactor, F is the total molar flow rate into the first reactor of the series combination, R_{N_2} is the rate of consumption of gaseous N_2 in step (2) (turnover frequency units, s^{-1}), and the designations "out" and "in" refer to the partial pressures at the outlet and inlet of each well-mixed reactor.

RESULTS OF KINETIC SIMULATIONS UNDER HIGH-PRESSURE CONDITIONS

The results of our kinetic simulations for the experimental condition of Nielsen are summarized in Figs. 1–4, in which we report the ammonia concentration (in %) as well as the fractional surface coverages by the predominant adsorbed species versus

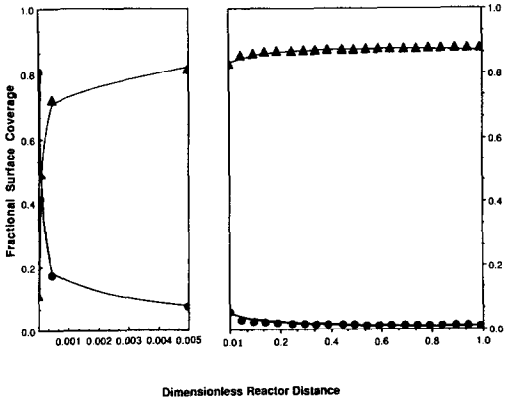

FIG. 2. Calculations, according to the model of Stoltze and Norskov, of fractional surface coverages by predominant adsorbed species versus dimensionless longitudinal distance from reactor inlet: (●) H*, (▲) N*.

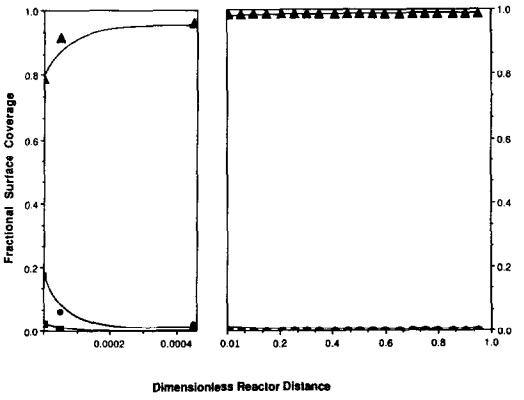

FIG. 4. Calculations, according to the model of Bowker *et al.* (Case 2), of fractional surface coverages by predominant adsorbed species versus dimensionless longitudinal distance from reactor inlet: (●) H*, (▲) N*, (■) N_2*.

TABLE 5

Comparison of Experimental Observations with Predictions from Kinetic Simulations for Ammonia Synthesis

Experiment: Observation	Experimental Value	Predicted value		
		Stoltze and Norskov	Bowker *et al.* (Case 1)	Bowker *et al.* (Case 2)
Nielsen (*21*)				
Ammonia concentration (%)	13.2	11.1	10.2	14.5
Dumesic *et al.* (*22*)				
Turnover frequency (s^{-1})	0.04	0.19	0.16	0.13
Topsøe *et al.* (*23*)				
Turnover frequency (s^{-1})	0.50	0.28	0.20	0.14
Spencer *et al.* (*9*)				
Turnover frequency (s^{-1})	12.7	60.0	25.0	40.0

longitudinal distance from the inlet of the plug-flow reactor. We have included these results versus reactor position to determine whether the nature of the most abundant reactive intermediate on the surface depends on the position of the catalyst in the reactor, as will be discussed later. The effluent ammonia concentrations predicted by the models of (1) Stoltze and Norskov, (2) Bowker *et al.* (Case 1), and (3) Bowker *et al.* (Case 2) are 11.1, 10.2, and 14.5%, respectively (see Fig. 1). This comparison is summarized in Table 5.

In Fig. 5, we report the departures from equilibrium for the slowest steps of the reaction mechanism versus longitudinal distance through the plug-flow reactor. The departure from equilibrium for a given step is defined as the ratio of the net rate of the step to the forward rate. This value approaches zero for an equilibrated step.

It can be seen that all three of the above

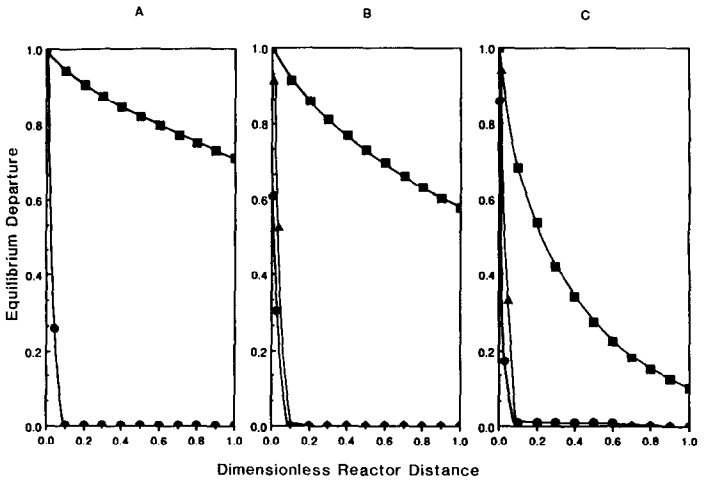

FIG. 5. Departure from equilibrium for slowest elementary steps in ammonia synthesis: (A) Stoltze and Norskov, (B) Bowker *et al.* (Case 1), (C) Bowker *et al.* (Case 2), (■) Step 2, (●) Step 3 in (A) and Step 5 in (B) and (C), ▲) Step 6.

kinetic simulations predict ammonia concentrations in the reactor effluent near the experimental value of 13.2%. Therefore, we conclude that it is possible to extrapolate successfully the results from single crystal studies to predict the performance of an industrial ammonia synthesis catalyst. According to Bowker *et al.* the use of the rate constants in Tables 2 and 3 should give ammonia concentrations of 3.0 and 5.4%, respectively. Indeed, we can obtain these values if we decrease the value of (PS/F) by a factor of 50. (This would correspond, for example, to a lower value of the site density or a lower catalyst density used by these authors.) Furthermore, at this lower value of PS/F, we find the same values of the surface coverages by adsorbed species as those reported by Bowker *et al.* We thus conclude that the difference betweeen the results of Stoltze and Norskov and those of Bowker *et al.* is due to different values of PS/F used by these authors. Our analysis of the reactor data of Nielsen agrees with the calculations of Stoltze and Norskov.

It is useful to comment on the results in Figs. 2–5. All three kinetic simulations agree that N* is the most abundant surface intermediate in the reactor, except at the reactor inlet where a variety of adsorbed species compete for surface sites (see Figs. 2–4). The results of all the kinetic simulations also agree with the well-known fact that the dissociation of dinitrogen (step 2) is slow (see Fig. 5). If the rate constants of Stoltze and Norskov are used, then the first hydrogenation of atomic nitrogen (step 3) is the next slowest step at the reactor inlet. In contrast, if the rate constants of Bowker *et al.* are used, then steps (5) and (6) involving NH_3* are the next slowest steps at the reactor inlet.

AMMONIA SYNTHESIS TURNOVER FREQUENCIES IN LABORATORY REACTORS

It was shown above that each of three models considered in this paper predicts adequately the ammonia concentration at the effluent of a commercial ammonia synthesis reactor operating at 107 atm. While this is an important result and shows the utility of the kinetic models under industrial reaction conditions, this experimental point does not provide a particularly sensitive test of the kinetic models, since the reactor is operating near equilibrium (i.e., the ammonia concentration at the effluent is 78% of the equilibrium value). Thus, a model that is consistent with the overall thermodynamics of ammonia synthesis may give a good prediction of the ammonia concentration leaving the reactor under the aforementioned conditions; however, this model may fail to provide a good estimate of the ammonia synthesis turnover at conditions far from equilibrium. We now address this problem in the present section with respect to the models of Stoltze and Norskov and Bowker *et al.* The comparisons that are presented below are summarized in Table 5.

Ammonia synthesis turnover frequencies were measured by Dumesic *et al.* (*22*) on various magnesia-supported iron catalysts at atmospheric pressure and conversions far from equilibrium. This reaction was found to be structure sensitive, with higher turnover frequencies observed for larger ion particles, which presumably exposed primarily (111) planes. The apparent turnover frequency for ammonia synthesis over large metallic iron particles was reported to be 0.04 s^{-1} in a stoichiometric H_2/N_2 gas mixture at a temperature of 678 K and at ammonia concentration equal to 20% of the equilibrium value. The reactor employed in these studies was a plug-flow reactor, and the apparent turnover frequency was calculated as the average number of ammonia molecules produced in the reactor per second per iron surface site as titrated by CO chemisorption. This value is described more correctly as a site time yield.

We have used the rate constants given in Tables 1–3 to predict the site time yields of ammonia at the conditions of Dumesic *et al.* The following values were obtained: 0.19 s^{-1} for the model of Stoltze and

Norskov, 0.16 s^{-1} for the model of Bowker *et al.* (Case 1), and 0.13 s^{-1} for Bowker *et al.* (Case 2). These values are at most a factor of 5 too high. This is considered to be good agreement when it is remembered that (i) the catalyst studied by Dumesic *et al.* was not promoted with potassium and (ii) CO chemisorption may overestimate the number of active sites.

Topsøe *et al.* (*23*) have used nitrogen chemisorption to titrate the active sites for ammonia synthesis on a series of metallic iron catalysts. Site time yields of ammonia were determined by these authors at 673 K using a stoichiometric H_2/N_2 gas mixture at atmospheric pressure and operating with an effluent ammonia concentration equal to 15% of the equilibrium value. The site time yield of ammonia reported for a potassium-promoted iron catalyst under these conditions was 0.5 s^{-1}. This value agrees well with the following predictions of the kinetic models addressed in the present paper: 0.28 s^{-1} for the model of Stoltze and Norskov, 0.20 s^{-1} for the model of Bowker *et al.* (Case 1), and 0.14 s^{-1} for Bowker *et al.* (Case 2). Furthermore, if nitrogen chemisorption does not necessarily titrate all of the active sites but instead this uptake is simply proportional to the active site density [as suggested by Topsøe *et al.* (*23*)], then the agreement between the experimental value of the turnover frequency and the predicted values becomes even better.

Spencer *et al.* (*9*) measured the turnover frequency for ammonia synthesis over an Fe(111) single crystal surface at a total pressure of 20 atm and a temperature of 748 K. For a stoichiometric H_2/N_2 gas mixture, the turnover frequency was determined to be 12.7 s^{-1}. The ammonia concentrations employed in this study were at most 10 Torr, i.e. less than 1.5% of the equilibrium concentration. Thus, these experiments provide a good test of ammonia synthesis kinetic models under conditions far from equilibrium.

When the three kinetic models of the present study are applied under the ammonia synthesis reaction conditions employed by Spencer *et al.*, we find that the turnover frequency depends on the ammonia pressure. This is due to an inhibition of the forward rate by ammonia, since the rate of ammonia decomposition is negligible under these experimental conditions. For an ammonia pressure between 5 and 10 Torr (typical values for the experiments reported), the following values of the ammonia synthesis turnover frequency are predicted by the kinetic models: 60 s^{-1} for the model of Stoltze and Norskov, 25 s^{-1} for the model of Bowker *et al.* (Case 1), and 40 s^{-1} for Bowker *et al.* (Case 2). The agreement of the predicted values with the experimental result is good, especially when it is noted that the Fe(111) surface studied by Spencer *et al.* did not contain potassium.

In summary, it can be seen in Table 5 that the kinetic models addressed in the present paper provide good predictions of the rate of ammonia synthesis over a range of temperatures (678–748 K), a range of pressures (1–20 atm), and a range of ammonia concentrations (1.5–20% of the equilibrium concentration). The success of these kinetic models in predicting the performance of an iron catalyst at 723 K and 107 atm was demonstrated in the previous section. Furthermore, two of these kinetic models [i.e., Stoltze and Norskov and Bowker *et al.* (Case 1)] provided adequate descriptions of the sticking coefficient for dissociative nitrogen adsorption and the temperature-programmed desorption spectra of nitrogen from the Fe(111) surface. We thus reach the remarkable conclusion that relatively simple kinetic models are able to reproduce nitrogen adsorption/desorption and ammonia synthesis behavior under conditions ranging from ultrahigh vacuum to 107 atm.

SIGNIFICANCE OF KINETIC MODELS

It is perhaps surprising that studies of adsorption/desorption phenomena on single crystal surfaces could be used to predict the turnover frequency for ammonia synthesis on iron catalysts under a wide range of ex-

perimental conditions. This is especially unexpected since any possible coverage dependence of the rate constants was not taken into account. Furthermore, it would appear to be difficult to determine the rate constants for the seven or eight elementary steps of the reaction mechanism with sufficient accuracy to conduct ammonia synthesis kinetic simulations with precision. In view of these considerations, why do the kinetic models addressed in this study work so well?

First, under all of the experimental conditions explored in the present paper, the dissociation of adsorbed dinitrogen (step 2) is the slowest step in the mechanism. [This is even true for the conditions of Spencer *et al.*, where the forward rate of step (2) is at least an order of magnitude slower than the forward rate of the next-slowest step.] In addition, adsorbed nitrogen is the most abundant nitrogen-containing surface intermediate in all cases. Thus, the rate constants of steps (3)–(9) are kinetically insignificant. It is sufficient for the purposes of predicting ammonia synthesis turnover frequencies to describe properly the kinetics and thermodynamics of nitrogen adsorption [steps (1) and (2)], and these are the steps that have been investigated in detail on single crystal iron surfaces. The estimates of the rate constants for steps (3)–(9) are used only to decide that these steps are, in fact, much faster than step (2) and that the surface coverages by NH_x species ($x > 0$) are small.

The possible effects of surface coverage on the rate constants of the ammonia synthesis mechanism are not known at present. It is important to note, however, that the surface coverage by atomic nitrogen is predicted by the kinetic models to be high under all of the experimental reaction conditions investigated in this paper. [For example, the lowest nitrogen coverage predicted by the model of Stoltze and Norskov and Bowker *et al.* (Case 1) is 0.4 for the experimental conditions of Spencer *et al.*] Thus, the rate constants reported by Stoltze and Norskov and Bowker *et al.* (Case 1) can be interpreted as being representative of surfaces covered primarily by atomic nitrogen. In fact, these are the conditions that were employed during the temperature-programmed desorption studies of iron single crystal surfaces. It is possible that the kinetic models would be less successful under conditions where the nitrogen coverage is very small or where atomic nitrogen is no longer the most abundant surface intermediate.

In closing, we note that it will be important in the future to continue the comparison of results of single crystal studies with results of studies carried out on high-surface-area catalysts under industrial reaction conditions. Studies of this nature are essential for kinetics-assisted catalyst design.

ACKNOWLEDGMENTS

We thank Haldor Topsøe A/S for support and encouragement during this project. We are particularly grateful to Per Stoltze and Jens Norskov for providing us with their estimates of the rate and equilibrium constants for the elementary steps involved in ammonia synthesis. Finally, we thank Professor D. F. Rudd for his interest, insight, and encouragement in catalyst design.

REFERENCES

1. Dumesic, J. A., Milligan, B. A., Greppi, L. A., Balse, V. R., Sarnowski, K. T., Beall, C. E. Kataoka, T., Rudd, D. F., and Treviño, A. A., *Ind. Eng. Chem. Res.* **26,** 1399 (1987).
2. Bowker, M., Parker, I., and Waugh, K. C., *Surf. Sci. Lett.* **197,** L223 (1988).
3. Stoltze, P., and Norskov, J. K., *Surf. Sci. Lett.* **197,** L230 (1988).
4. Ertl, G., "Critical Reviews in Solid State and Materials Science," p. 349. CRC Press, Boca Raton, FL, 1982.
5. Grunze, M., *in* "The Chemistry and Physics of Solid Surfaces and Heterogeneous Catalysis" (D. A. King and D. P. Woodruff, Eds.), Vol. 4, p. 413. Elsevier, Amsterdam, 1982.
6. Grunze, M., Golze, M., Hirschwald, W., Freund, H. J., Pulm, H., Seip, H., Kuppers, J., and Ertl, G., *Phys. Rev. Lett.* **53,** 850 (1984).
7. Ertl, G., *in* "Catalysis, Science and Technology" (J. R. Anderson and M. Boudart, Eds.), Vol. 4, p. 208. Springer-Verlag, Berlin, 1983.

8. Ertl, G., *Catal. Rev. Sci. Eng.* **21,** 201 (1980).
9. Spencer, N. D., Schoonmaker, R. C., and Somorjai, G. A., *J. Catal.* **74,** 129 (1982).
10. Spencer, N. D., Schoonmaker, R. C., and Somorjai, G. A., *Nature (London)* **294,** 1643 (1981).
11. Grunze, M., Golze, M., Fuhler, J., Neumann, M., and Schwartz, E., *in* "Proceedings, 8th International Congress on Catalysis, Berlin," Vol. 4, p. 133. Verlag Chemie, Weinheim, 1984.
12. Ertl, G., Grunze, M., and Weiss, M., *J. Vac. Sci. Technol.* **13,** 314 (1976).
13. Boszo, F., Ertl, G., Grunze, M., and Weiss, M., *J. Catal.* **49,** 18 (1977).
14. Boszo, F., Ertl, G., Grunze, M., and Weiss, M., *Appl. Surf. Sci.* **1,** 103 (1977).
15. Weiss, M., Ertl, G., and Nietsche, F., *Appl. Surf. Sci.* **2,** 614 (1979).
16. Ertl, G., Lee, S. B., and Weiss, M., *Surf. Sci.* **114,** 527 (1982).
17. Stoltze, P., and Norskov, J. K., *Phys. Rev. Lett.* **55,** 2502 (1985).
18. Stoltze, P., *Phys. Scr.* **36,** 824 (1987).
19. Stoltze, P., and Norskov, J. K., *J. Catal.* **110,** 1 (1988).
20. Bowker, M., Parker, I., and Waugh, K., *Appl. Catal* **14,** 101 (1985).
21. Nielsen, A., "An Investigation of Promoted Iron Catalysts for the Synthesis of Ammonia." Gjellerup, Copenhagen, 1968.
22. Dumesic, J. A., Topsøe, H., Khammouma, S., and Boudart, M., *J. Catal.* **37,** 503 (1975).
23. Topsøe, H., Topsøe, N., Bohlbro, H., and Dumesic, J. A., *in* "Proceedings, 7th International Congress on Catalysis" (T. Seiyama and K. Tanabe, Eds.), p. 247. Elsevier, New York, 1980.